Ordering of agarose near the macroscopic gelation point

Donatella Bulone,[1] Daniela Giacomazza,[1] Vincenzo Martorana,[1] Jay Newman,[2] and Pier L. San Biagio[1]
[1]*CNR Institute of Biophysics, Via Ugo La Malfa 153, I-90146 Palermo, Italy*
[2]*Department of Physics, Union College, Schenectady, New York 12308, USA*
(Received 29 July 2003; published 14 April 2004)

Gel formation and spatial structure is an important area of study in polymer physics and in macromolecular and cellular biophysics. Agarose has a sufficiently complex gelation mechanism to make it an interesting prototype for many other gelling systems, including those involved in amyloid fibrillogenesis. Static (over a scattering vector range of $0.1-30\ \mu m^{-1}$) and dynamic light scattering and rheology methods were used to follow the gelation kinetics of agarose at 0.5% in water or in the presence of 25 m*M* NaCl and quenched to temperatures of 20–43 °C. Light scattering results on gelling samples are fully described by a fractal aggregate model with four physically meaningful parameters. In all cases aggregates, with fractal dimensions at or near 3, form more rapidly and are smaller in characteristic size at lower quench temperatures. A region three to four times larger than the aggregate becomes depleted of agarose as the gelation proceeds. Below about 30 °C the aggregation process freezes spatial ordering rapidly, resulting in fragile macroscopic gels as determined by rheology. Salt effects are seen to be minimal and not important in the fundamental aggregation mechanism.

DOI: 10.1103/PhysRevE.69.041401 PACS number(s): 82.70.Gg, 83.80.Kn, 82.35.Lr, 82.35.Jk

I. INTRODUCTION

Gel structure and formation is a subject of increasing interest and importance, especially in cellular and subcellular biology, but also in the more general area of polymers [1–3]. Often the process of gel formation is a multistep one exhibiting hysteresis and leading to a variety of final structures depending on the particular solvent and environmental conditions [4–10].

From many different gel systems that have been studied using a large variety of physical methods, some common features of hydrogel formation have been elucidated. Gelation is often the result of competition between different and mutually interacting processes, such as a conformational change, molecular cross-linking, and liquid-liquid phase separation [11–14]. The latter occurs when the solution is brought either in its thermodynamically unstable region (spinodal demixing) or in its metastable region (nucleated demixing). Experiments and computer simulations have shown that the structural properties of gels, formed under appropriate conditions, are strongly dependent on the relative time scales of the processes involved [15–19]. The kinetics of these processes can be tuned by changing the quenching temperature, polymer concentration, and solvent composition.

In this study, we use laser light scattering and rheology techniques to investigate the formation and structure of agarose gels at 0.5% w/v, which is a concentration near the threshold for overlap of agarose random coils [20]. Agarose is a well-characterized biostructural polysaccharide obtained from marine seaweed [21]. It provides a simple suitable system for studying the *in vitro* self-assembly of polymer networks and its dependence on environmental parameters. Here we examine the gelation kinetics of agarose in water and in the presence of small amounts of monovalent salt (NaCl) as probed by low-angle and standard static light scattering, dynamic light scattering, and rheology, in order to study the process in more detail and to look for any charge screening effects of salt on the formation kinetics and structure of these gels.

Previous publications from our laboratory have reported on measurements of agarose in aqueous solution under a variety of conditions, so providing a phase diagram indicating the type of gelation mechanism to be expected depending on the quenching temperature and polymer concentration [8]. At low to moderate agarose concentrations (up to about 1% w/w), solution demixing is the first event in the sequence of processes leading to polymer self-assembly. Quenching of the polymer solution inside its instability region causes demixing into regions of higher and lower concentration [8,20,22,23]. Inside the polymer rich regions, molecular cross-linking can start and a macroscopic gel is obtained if the average concentration is large enough to warrant percolation, or cross-linking, between these high concentration regions. The long-range structure of gel formed under these conditions will reflect the spatial order imposed by the demixing process on the arrangement of mutually connected polymer clusters. At very low concentrations of 0.01–0.05%, usually reported as nongelling concentration, evidence was presented for gelation actually occurring on a mesoscopic scale [24–26]; high concentration regions generated by solution demixing remain mutually disconnected and freely diffusing in a sample that appears macroscopically liquid. At concentrations larger than 1%, strong competition between kinetics of demixing and cross-linking are expected [27] and indeed observed [15]; very different gel structures can be obtained at fixed polymer concentration by changing the quenching temperature [15], the major difference being that no trace of large scale ordering is seen at low temperature, where the rapid cross-linking process completely inhibits solution demixing [15].

At the agarose concentration used in the present work, the cross-linking process requires the occurrence of solution demixing; therefore, in gels formed at any temperature, the long-range solution ordering is imposed by demixing. The effects of the competition between the two processes are reflected in the kinetics of gelation and in the structural prop-

erties of the gel. Static light scattering data as a function of quench temperature (20–43 °C) and scattering angle (0.1°–150°, corresponding to inverse scattering vectors ranging from 0.04 to 50 μm) have been analyzed using a model where fractal aggregates composed of identical subunits are surrounded by a region depleted of polymer. Six model parameters include the subunit and the aggregate sizes and fractal dimensions, the depletion region size around the aggregate, and the intensity amplitude, proportional to the aggregate mass per unit volume. These, together with viscoelastic moduli, allow us to interpret our data in terms of the spatial ordering of connected polymer clusters.

II. MATERIALS AND METHODS

The agarose used in our experiments was Seakem HGT(P) agarose, purchased from BioProducts Marine Colloid Division, having a low sulphate content ($<0.15\%$). Previous dynamic light scattering experiments [20] have found that this material is fairly monodisperse (average molecular weight$=120$ kD$\pm 10\%$). The agarose powder was dissolved in Millipore (SuperQ) water for 20 min at 100 °C, and filtered at 80–90 °C through 0.22 μm Millipore filters before any measurements. For light scattering measurements the agarose sols were filtered directly into preheated optical cuvettes, sealed, and quenched to the measurement temperature by immersing them in a thermostated bath.

Viscoelastic measurements were made using a TA Instruments AR 1000 rheometer with cone (4 cm diameter, angle $<1°$)-plate geometry. Measurement temperature was controlled by a Peltier system. Measurements were made at various quenching temperatures in the range between 43 and 20 °C using a protocol that first monitored the elastic and viscous moduli as functions of time for periods of 2 h at low frequency and strain (0.1 Hz and 4×10^{-3}, respectively). Then frequency spectra were recorded over more than three decades (0.01–30 Hz), with the same strain so as not to disrupt the gels. Finally, the strain was varied (4×10^{-3}–200), while the frequency was kept fixed at 1 Hz, to disrupt the gel while monitoring the elastic and viscous moduli. To avoid too rapid gelation at the lower quench temperatures while loading the samples, which might lead to nonuniform gel formation, the samples were loaded with the rheometer plate kept at 60 °C and then rapidly brought to the quench temperature.

Light scattering measurements at scattering angles above 10° were performed using cylindrical sample optical cuvettes immersed in the thermostated optical bath of a Brookhaven Instruments BI-200SM goniometer. Either a Spectra Physics argon ion laser tuned at $\lambda=514.5$ nm or a Spectra Physics 127 helium-neon laser at 632.8 nm was used as a light source. A BI-2000 correlator was used to obtain static and dynamic light scattering data for scattering angles θ between 10° and 150°, corresponding to scattering vector magnitudes q between 2.3 and 25 $\mu\mathrm{m}^{-1}$, where $q=4\pi n\lambda^{-1}\sin(\theta/2)$ with n equal to the index of refraction of the solvent. Dynamic light scattering measurements on nonergodic gel samples were made while scanning different regions of the sample using a motor-driven cell holder so that ensemble averages were obtained [28].

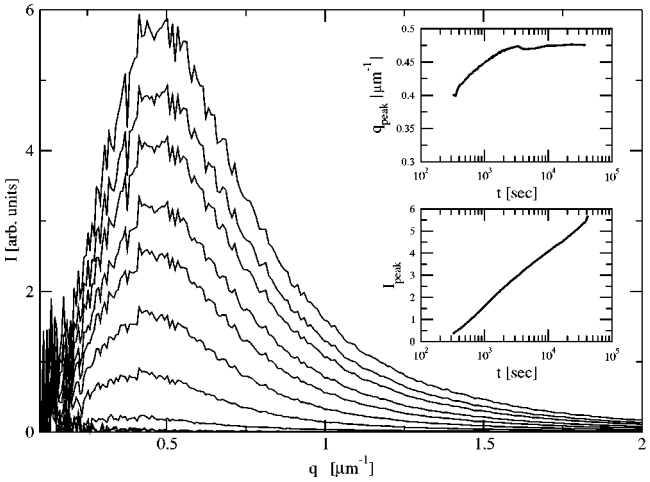

FIG. 1. Intensity vs q for 0.5% agarose in water quenched to 38 °C. The curves shown are plotted at equal steps in $\log t$. The upper inset shows the position of the peak as a function of time, while the lower inset shows the peak intensity as a function of time.

Low-angle light scattering measurements were performed using a 30 mW Melles Griot helium-neon laser and a charge coupled device (CCD) Pulnix TM765 camera. The system was constructed following published work [29]. Measurable intensities range from 1.0 to 3×10^5 (in arbitrary units), thanks to a software integration of multiple exposure times (1/60–1/10 000 sec). After background subtraction (using software), reliable measurements could be made over a range of scattering angles of 0.1°–11°, corresponding to scattering vector magnitudes of 0.02–2 $\mu\mathrm{m}^{-1}$, with a maximum resolution of 0.01°.

III. RESULTS

A. Agarose at 0.5% in water

Agarose samples prepared at 0.5% (w/v) and 80–90 °C were quenched to various temperatures in the range of 20–43 °C and the scattered light from the samples was monitored using both standard static light scattering and low-angle static light scattering. These temperatures are all below the spinodal temperature measured for this concentration of agarose, 49.8 °C [20,30–31]. As a point of reference, note that at this agarose concentration the onset of macroscopic gelation is observed to occur after about 300 min at a quenching temperature of 47.5 °C. Figure 1 shows representative data for the low-angle light scattering intensity I vs q as a function of time following a quench to 38 °C. Note that the different curves shown were selected at logarithmically spaced time intervals. A peak in the intensity is apparent a few minutes after the quench, indicating a pattern of regions of higher- and lower-than-average agarose concentration. The insets show the shift in peak position and peak intensity as functions of time after the quench. We are not able to follow the expected exponential growth of the scattered light intensity just after the quench both because of the very fast

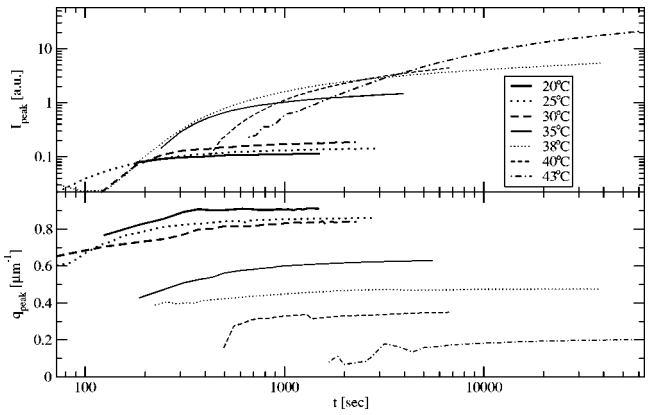

FIG. 2. Scattering peak positions (upper) and intensities (lower) as functions of time for samples of 0.5% agarose in water quenched to different temperatures.

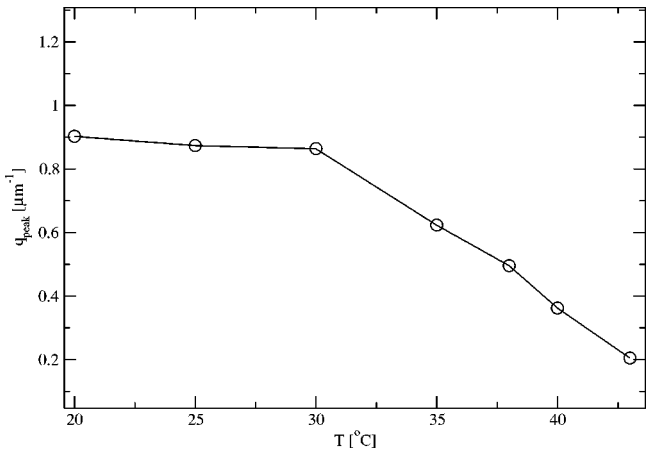

FIG. 3. Peak positions at 0.5 h after quench as a function of quench temperature for 0.5% agarose in water.

kinetics of the initial demixing under the chosen experimental conditions as well as the low sensitivity of the CCD camera.

The top inset shows that over a period of minutes the peak shifts toward larger q, increasing by about 20% and remaining stable after about 1 h. The length corresponding to the peak position, $L_{\max}=2\pi/q_{\max}$, decreases from 16 to 13 μm over 1 h. The bottom inset shows that the peak intensity increases roughly logarithmically with time, indicating that the rate of increase in intensity steadily decreases with time (since $I\sim\ln t$ implies that $dI/dt\sim 1/t$).

Figure 2 shows the normalized peak intensities (top) and the peak positions (bottom) as a function of time for different quench temperatures for a set of identically prepared agarose samples in water at a concentration of 0.5%. Both parameters vary systematically with quench temperature: $q_{\max}$ values decrease with increasing quench temperature and plateau or long-time $I_{\max}$ values increase with increasing quench temperature. For quenches of 30 °C or below, the kinetics are fast with the peak position and intensity reaching a similar plateau within about 10 or 20 min. Above 30 °C, there is a shift in peak position toward smaller q, an observed lag time in peak intensity growth (at least with our detector's sensitivity), as well as a much slower growth in intensity, which at the highest temperature has not reached a plateau even after 15 h.

In Fig. 3 we show the final peak position after 0.5 h as a function of the quench temperature. Note that there again appear to be two regimes: below 30 °C, where the final q_{peak} remains at about 0.9 μm independent of the quench temperature, there is no apparent lag time (see Fig. 2) and the peak intensity does not increase further after a few minutes, as if the spatial decomposition giving rise to the peak scattering becomes frozen in time and above 30 °C, where there is a steady decrease in q_{peak} with increasing temperature, an increasing lag time and a slower but steady increase in peak intensity that reaches greater intensities with increasing quench temperature.

These spectra can be characterized by, in addition to the peak position and intensity, the q dependence of the intensity in the higher q tail portion of the spectrum. We find a power law dependence due to a variation in the structure function $S(q)$ (see below) as

$$S(q)\propto q^{-d_f}, \tag{1}$$

with d_f equal to the fractal dimension of the agarose sample [4]. Log-log plots of these data show a similar dependence at all quench temperatures. By scaling the peak position and peak intensity for agarose samples quenched to different temperatures we see in Fig. 4 that the q dependence at larger q in the low-angle light scattering data appears to be independent of quench temperature. The negative of the slopes of the log-log plots, the fractal dimension, is equal to about 3.0, nearly independent of quench temperature for agarose at 0.5%, indicating compact scatterers giving rise to this portion of the spectrum.

Static light scattering using the Brookhaven Instruments system on identically prepared samples gave similar results to those at smaller scattering angles. Time courses of intensity growth at $q=18.7$ μm^{-1} at various quench temperatures were quite similar to those at smaller q with intensity data at

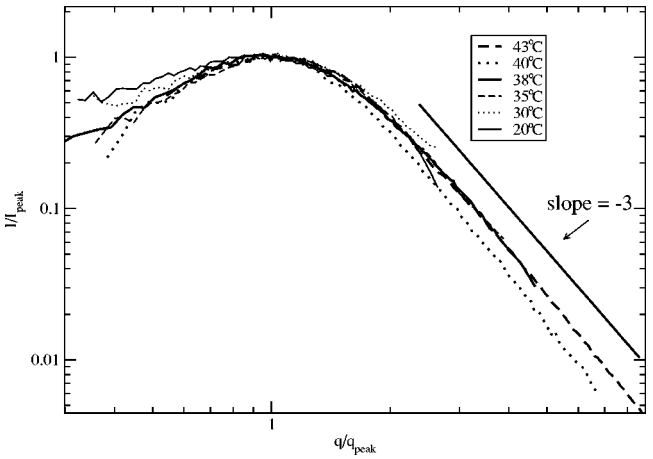

FIG. 4. The q dependence of the scattered intensity for 0.5% agarose quenched to different temperatures. The different curves were scaled to match the peak positions both in I and in q in order to compare the slopes at the higher q values.

or below 30 °C reaching a plateau within about 10 min and intensities at 43 °C increasing steadily and not reaching a plateau even after 15 h. Linear $\log I$ vs $\log q$ plots were obtained over the full accessible range of q ($2.3–25\ \mu m^{-1}$) with slopes equal to about 1.4 above 30 °C, and somewhat smaller, about 1.0, at lower quench temperatures. These values are approximately half those found using the low-angle light scattering system over a lower range of q values ($0.5–2.0\ \mu m^{-1}$). We have attempted to combine these data with those at low angle in order to analyze them together with a comprehensive model in a section below.

Dynamic light scattering experiments were performed on 0.5% agarose solutions at a higher temperature (55 °C), above the spinodal, where the sample is in a stable sol state. The intensity autocorrelation functions were well fit by double exponentials with a smaller component of 10–15 nm and a larger component of 100–150 nm, consistent with previously published results [20]. Similar experiments on samples quenched below the spinodal temperature are complicated by the formation of microscopically inhomogeneous gels. By using a smaller detector aperture and by scanning the sample cuvette in order to ensemble average [28], we simultaneously measured the average scattered intensity and autocorrelation function on a sample quenched to the higher limit of our temperature range (43 °C), in an attempt to follow the change in the dynamics of the system. The quality of the autocorrelation function, due to its rapid change, did not allow an accurate data analysis. Only an average relaxation time was obtained from a cumulant analysis, showing a steady and rapid increase in the first 20–30 min in parallel with a similar increase in the intensity. After that time both the average intensity and relaxation time fluctuated wildly (by over 100%) due to the onset of a gel network.

Rheology measurements were performed on a series of 0.5% agarose samples quenched to temperatures below the spinodal. At temperatures of 30 °C or below, within the 5 min required for thermal equilibration the elastic (and viscous) moduli measured at low strain and frequency had reached nearly common high plateaus (with slightly smaller elastic moduli for samples quenched to higher temperatures, all below 30 °C). Above 30 °C, elastic moduli increased with a time course that was similar to that for the scattered intensity of light at the same quench temperature; the elastic modulus plateau at 38 °C is over ten times smaller than those below 30 °C while at 43 °C, a plateau is not reached even after 15 h but the elastic modulus value is more than 2000 times smaller than those below 30 °C, as shown in Fig. 5 (a).

Following the rheology time course measurements, mechanical spectra were performed, varying the frequency while keeping the strain low. Spectra [shown in panel (b) of Fig. 5] at lower temperatures were flat indicating strong gels while those at the highest temperatures showed some decrease in moduli at the lowest frequencies, indicating a weaker network with relaxation time of the order of 50–100 sec. For each sample a subsequent low frequency increase of the applied strain led to a rupture of the gel network. Gels formed at higher quench temperatures are more resistant to breakage (requiring larger strains by a factor of about 3) than those formed at lower temperatures, even though they have lower elastic moduli.

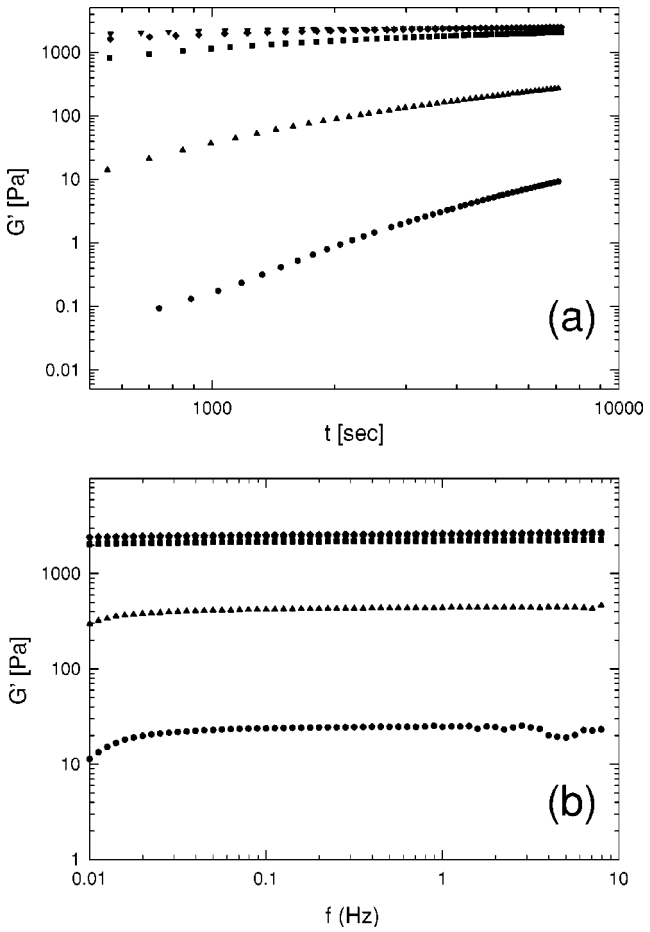

FIG. 5. (a) Time dependence of the elastic modulus (G') for 0.5% agarose in water at different quenching temperatures. Circles = 43 °C; triangle up = 38 °C; squares = 30 °C; diamonds = 25 °C, and triangle down = 20 °C. (b) Mechanical spectra measured at the end of rheology time course experiment shown in (a). Same symbols as in (a).

B. Effects of salt

When 0.5% agarose samples are prepared in the presence of 25 m*M* NaCl and quenched to various temperatures, low-angle static light scattering results differ from those in the absence of salt in a number of ways. A peak is still observed at forward scattering angles, but it is shifted to smaller q values by about 10% at all quench temperatures. The peak intensity grows faster (having a shorter, or no apparent, lag time but similar kinetics to samples of 0.5% agarose in water) and, at the lower quench temperatures, to higher levels than in the absence of salt. Below 30 °C the kinetics are very rapid and within about 10 min the intensity in the presence of salt has increased and reached a plateau at about five times more scattered intensity than in the absence of salt. Above 30 °C, with slower kinetics, although the scattered intensity is larger in the presence of salt, the ratio of scattered intensity in the presence of salt to that in its absence decreases very

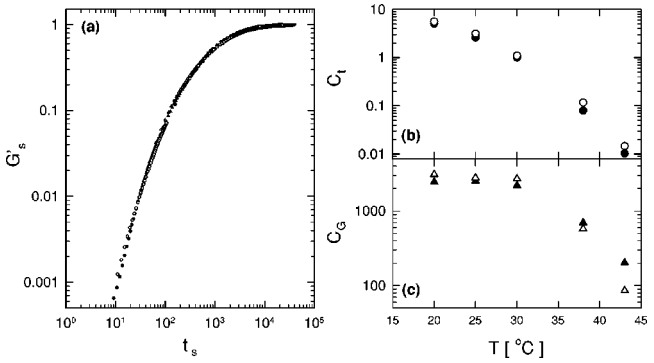

FIG. 6. (a) Scaled elastic moduli data for 0.5% agarose at $T=20$, 25, 30, 38, and 43 °C in water (solid symbols) and in the presence of 25 mM NaCl (open symbols). The G_s' plateau at long times has been arbitrarily set to 1. (b) Time (C_t) (circles) and (c) $G'(C_G)$ (triangles) coefficients used for the scaling shown in (a) for 0.5% agarose in water (solid symbols) and in the presence of 25 mM NaCl (open symbols).

slowly towards a value of 1.0. The exponent of the power law dependence of the structure factor in the presence of 25 mM NaCl (not shown) is about 3 at all quench temperatures, as in the absence of salt.

Static light scattering at larger q values yields linear data for $\log I$ vs $\log q$ with fractal dimensions of 1.5, independent of quench temperature, again roughly half the value determined at smaller q values by low-angle light scattering. The difference in the q dependence for the two different ranges of q is discussed in the following section on a model used in the analysis of both sets of light scattering measurements. Mean radii of agarose species from dynamic light scattering experiments at high temperature (55 °C) in the presence of 25 mM NaCl were slightly ($\sim$25%) larger than in the absence of salt.

Rheology experiments showed that the salt addition has very little effect on the gelation kinetics. Typically, elastic moduli were slightly larger in the presence of salt at lower quench temperatures, but equal or smaller at the higher quench temperatures. A master curve can be obtained after scaling of the kinetics performed at different quenching temperatures (20, 25, 30, 38, and 43 °C) either in the presence or absence of NaCl, as shown in Fig. 6(a). This indicates the existence of a unique process responsible for the increasing elastic modulus. Figures 6(b) and 6(c) show the scaling coefficients for time (C_t) and G' (C_G), respectively. Temperature effects on both parameters are very strong; in fact, at increasing temperature, C_t follows a diverging law reflecting the slowing down of the aggregation process; C_G remains constant up to 30 °C and then decreases with an overall behavior qualitatively similar to the q_{peak} dependence on temperature shown in Fig. 4. The differences between C_t or C_G in the presence and absence of NaCl, at each temperature value, are very small suggesting that the salt does not affect the process involved in the agarose self-assembly. Strains required to rupture gels (at all quench temperatures) were also slightly higher in the presence of salt (data not shown).

C. Model for light scattering results

Even though many of the characteristics of a spinodal decomposition are missing from our data, it is reasonable to expect that an initial decomposition does take place, as previously shown in the case of higher agarose concentrations [16]. In fact at the lower agarose concentration here studied, the initial linear stage of the spinodal decomposition is not experimentally accessible because the peak of the structure factor falls at a lower q value, where the sensitivity of the CCD camera is insufficient to detect the faint signal of the early time growth of the structure factor over the stray light due to the transmitted laser beam.

Thus we believe that under our experimental conditions we are observing the late stage of the decomposition. In contrast to the usually observed coarsening of the solution, we observe a peak that, if anything, moves towards larger q. It is clear that the concurrent process of cross-linking is interfering with the expected ripening of the high concentration regions formed under the decomposition.

It is also clear from our data, and also from data in the literature [27], that such competition/interference is strongly and nonlinearly dependent on quench temperature. In view of such complexity we wish to find a semiphenomenological description, as opposed to a "first-principles" description [32,33], capable of fitting our low-angle light scattering data at all quenching temperatures and times.

A phenomenological model must have a self-similar tail at high q and a central peak going to a very low intensity for $q\rightarrow 0$. The large q behavior, describing the internal structure of the high polymer concentration regions, can be taken into account by using a model for monodisperse aggregates with N aggregates per unit volume, each composed of the same number n of identical subunits of mass m [34]. The excess scattered intensity, over that of the solvent, is proportional to the product of the static structure factor $S(q)$ due to the ordering of subunits within a single aggregate and the form factor $P(q)$ of the subunit, and is given by

$$I(q)=KN(nm)^2S(q)P(q), \tag{2}$$

where K is an experimental constant depending on the optics and the refractive index difference between the scatterers and the solvent. The aggregates are defined by both a characteristic size ξ and a fractal dimension d_f. An additional parameter r_o gives the distance $2r_o$ between nearest-neighbor subunit centers of mass. Assuming an exponential external cutoff in the pair-correlation function of the aggregate,

$$g(r)=\frac{d_f}{4\pi r_0^{d_f}}r^{d_f-3}e^{-r/\xi}, \tag{3}$$

the static structure factor can be obtained analytically [34] for $qr_o\ll 1$ and $\xi\gg r_o$ as

$$S(q)=\frac{1}{n}[1+F(q)]$$

$$=\frac{1}{n}\left[1+\frac{d_f\Gamma(d_f-1)\sin[(d_f-1)\arctan(q\xi)]}{(qr_o)^{d_f}\left(1+\frac{1}{q^2\xi^2}\right)^{(d_f-1)/2}}\right], \tag{4}$$

where Γ denotes the Gamma function and the division by n ensures the correct limiting behavior of $S(q)$ for $q\to 0$, since, by definition [34], $n-1=\int_0^\infty 4\pi r^2 g(r)dr = F(q\to 0)$.

This model does account for the large q value behavior of our data, but does not provide any peak. The presence of a peak could be attributed to the correlation/interaction between regions of high and low concentration [35] and/or to an anticorrelation effect due to depletion of the region close to the cluster [36]. Initially we tried to introduce a simple excluded volume kind of interaction in a multiplicative way in Eq. (2), and then tried to use the full expression for the hard spheres structure factor. The best fit was generally poor and required the use of parameters with little physical justification, such as a very high volume fraction (to adjust for the small q behavior) and a hard sphere radius much larger than the aggregate size ξ (to adjust for the peak position).

We then investigated the introduction of a depletion term in $g(r)$. Depletion would be relevant if polymer diffusion gets so low that clusters grow at the expense of nearby material. To account for the depletion region surrounding the aggregate, we introduce a negative correction term in the pair-correlation function so that the integral of $[g(r)-1]$ over the volume vanishes, in turn imposing the condition that $S(q=0)=0$. The correction term should be (i) smooth over the ξ distance scale to limit its influence to the small-q region and (ii) analytically tractable. We choose the correction term in $g(r)$ to be proportional to a Gaussian function:

$$g(r)=\frac{d_f}{r_0^{d_f}}\left[\frac{r^{d_f-3}e^{-r/\xi}}{4\pi}-\frac{\xi^{d_f}\Gamma(d_f)}{\pi^{3/2}R^3}e^{-(r/R)^2}\right], \qquad (5)$$

where $R\gg\xi$ is the characteristic size of the depletion region, and the prefactor enforces mass conservation. Note that when this depletion effect is not relevant, that is, in the limit $R\to\infty$, Equation (5) reduces to Eq. (3). The corresponding structure factor is then given by $S(q)=n^{-1}[1+F(q)-G(q)]$, where $G(q)=\Gamma(d_f+1)(\xi/r_o)^{d_f}e^{-(qR/2)^2}$.

The excess scattered intensity due to the aggregates is therefore given by

$$I(q)=KCm^2P(q)[1+F(q)-G(q)], \qquad (6)$$

where $C=N\ n$ is the number concentration of subunits and the correction $G(q)$ is only significant for small q and leads to a decrease in $I(q)$ at low q from the typical low-angle plateau. Note that in the limit of $q\xi\gg 1\gg qr_o$ this reduces to

$$I(q)=KCm^2P(q)\{d_f r_0^{-d_f}\Gamma(d_f-1)\sin[\pi(d_f-1)/2]\}q^{-d_f} \sim q^{-d_f}, \qquad (7)$$

giving the power law dependence used above in Eq. (1) at larger q in the direct fitting for d_f.

For the form factor $P(q)$ describing the subunit structure, we use the so-called Fisher-Burford form factor [37]:

$$P(q)=\frac{1}{\left[1+\frac{q^2r_0^2}{(3D_f/2)}\right]^{D_f/2}}, \qquad (8)$$

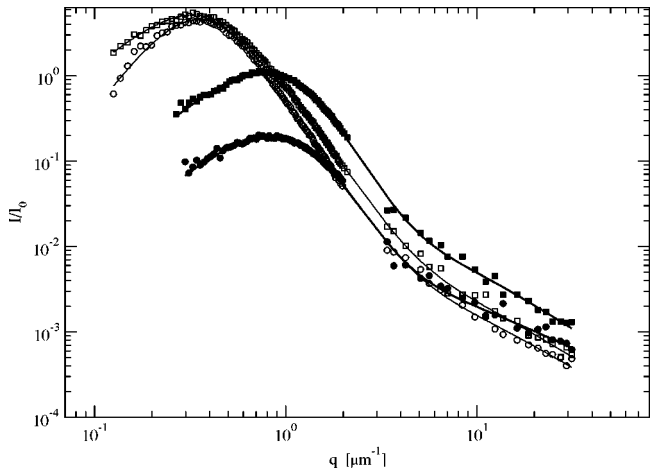

FIG. 7. A composite of the low- and high-angle data for 0.5% agarose as a function of q. The data are for temperatures $T=40$ (open circle—water; open square—25 mM NaCl) and 30 °C (full circle—water; full square—25 mM NaCl). The smooth curves shown are the fits to Eq. (6).

where we have used the same r_o value for the subunit effective radius and have assumed a second fractal dimension D_f for the subunit.

The complete expression for the intensity in this model thus depends on six parameters: the amplitude ($M=KCm^2$), proportional to the total aggregate mass per unit volume, the aggregate characteristic size ξ, the subunit characteristic radius r_o, the depletion region characteristic size R, and the fractal dimensions of the aggregate d_f and of the subunit D_f. Note that in principle changes in M could be due either to changes in the number of aggregates and/or in the number and density of subunits within the aggregates.

In order to combine both our low-angle and high-angle static light scattering data in the same graph of $I(q)$ so that we can test this model we need an intensity standard that can be used to calibrate the relative efficiencies of the two different optical systems. Note that with our current system there is a small range of q for which we have no data, making this calibration necessary. At this point, lacking such a calibration standard, we have scaled all the high-angle data together with one single additional parameter in order to be able to plot these data together as in Fig. 7. Then these data were directly fit to Eq. (6) in order to determine the six parameters of this model for 0.5% agarose solutions quenched to various temperatures. The smooth lines in Fig. 7 show the quality of these fits. Fitting parameters r_o and D_f of this model at the two different quench temperatures of the figure in the presence and absence of 25 mM NaCl range between 0.2 and 0.28 μm and between 1 and 1.5, respectively.

As an alternative fitting method, we separately fit the low-angle and the high-angle data. The lower-angle data, which provide a time-resolved description of the system, were fit to Eq. (6), but with $P(q)$ taken to equal 1.0 for this range of q, reducing the number of free parameters to four: d_f, ξ, R, and the intensity amplitude M. Since the other parameter r_o

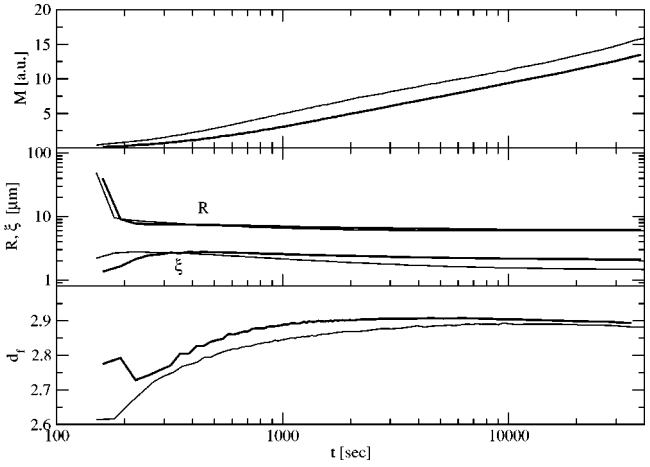

FIG. 8. Time evolution of the four parameters obtained from a fit of the low-angle data to Eq. (4) with $P(q)=1$ for 0.5% agarose quenched to 38 °C (thick lines—in water; thin lines—in 25 mM NaCl).

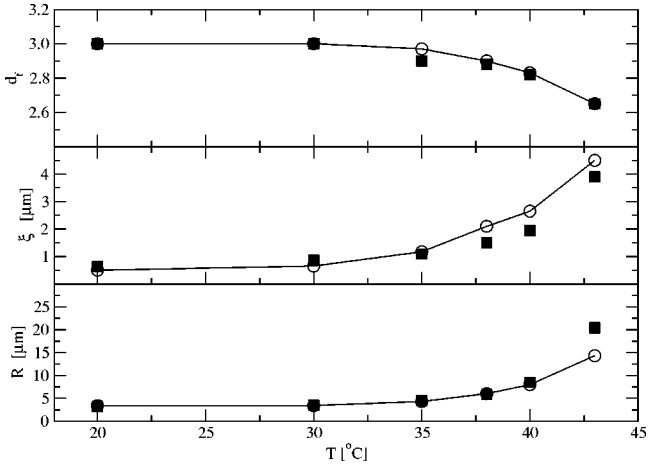

FIG. 9. The infinite-time extrapolated fitting parameters d_f, the aggregate fractal dimension, ξ, the aggregate characteristic size, and R, the depletion zone characteristic size, as functions of the quench temperature for 0.5% agarose in water (open circles+line) and in 25 mM NaCl (full squares).

affects low-angle data very slightly, we choose to fix it at 0.25 μm, consistently with previous measurements [38]. Application of this alternative fitting approach yields fit parameters d_f, ξ, R, and M very close to those obtained above.

In Fig. 8 the time evolution of the four parameters is shown for data at 38 °C. Kinetic data were fit in batch, recursively, starting from the final time where the signal-to-noise ratio is larger. The amplitude parameter M is very well described as increasing proportionately with the logarithm of the time after the quench, as seen directly in the bottom inset of Fig. 2. An initial growth and a subsequent small condensation of the aggregate size also are seen to occur over this time with a fractal dimension rapidly approaching and remaining at a value of about 2.9. Depletion zone characteristic dimensions decrease monotonically with time in parallel with those of the aggregates but always remaining three to four times greater than ξ. It is worth noting that, for all temperature quenches, at very short times, but after ξ has set in, R abruptly decreases to a relatively small value indicating that the depletion effect becomes relevant. As remarked above, this indicates the onset of the slowing down of subunit diffusion. The kinetics results show that the intensity amplitude M increases as the aggregate mean size shrinks only slightly.

In Fig. 9 the values of the aggregate fractal dimension, its characteristic size, and that of the depletion zone are shown as functions of the quench temperature for samples both with and without added salt. These values were obtained from an extrapolation to infinite time. Below 35 °C, the fractal dimension is 3.0, while the characteristic aggregate size grows slightly from just under 0.5 μm to about 1 μm, for agarose in both solvents. At 40 °C and above, the fractal dimension decreases slightly to a low of almost 2.6, while the characteristic aggregate size grows to at most 4.5 μm. The depletion zone characteristic size R behaves similar to ξ, going from 3 μm at low temperatures to 20 μm at 43 °C in the presence of salt. Thus, the depletion zone is consistently much larger than the aggregate size at any quench temperature. The ratio between R and ξ (not shown) increases as the quench temperature is lowered, in agreement with a faster and stronger cross-linking process.

Extrapolation to infinite time is more problematic in the case of the intensity amplitude M due to its logarithmic growth at later times, at least for temperatures above 30 °C. In Fig. 10 we report the profiles of M vs t at all quench temperatures with or without added salt. The growth of M occurs in a first, faster, stage where most of the signal builds up, and a second logarithmic-like stage that, for $T>30$ °C, lasts for times longer than the experiment duration. The solution with added salt exhibits a more rapid initial growth at all quench temperatures. From the log-log scale of Fig. 10, it is apparent that there exits a common asymptotic value of M for both sets of data, with the NaCl containing solutions tending to a slightly larger value. During the lower tempera-

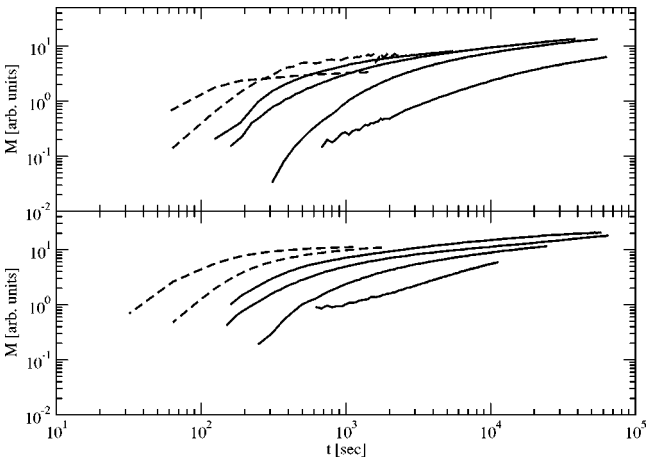

FIG. 10. Time evolution of the aggregate mass M for quench temperatures $T=20$, 30, 35, 38, 40, and 43 °C (from left to right), for 0.5% agarose in water (top panel) and in 25 mM NaCl (bottom panel). The profiles at lower quench temperatures (20 and 30 °C) are indicated with dashed lines.

ture quenches ($\leqslant 30\,^{\circ}\mathrm{C}$) the intensity amplitude M rapidly reaches plateau values that are somewhat smaller than the expected asymptotic values for temperatures $> 30\,^{\circ}\mathrm{C}$.

IV. DISCUSSION

Agarose is an interesting prototype hydrogel system that has a rich phase diagram. Using low-angle and standard static and dynamic light scattering, as well as rheology, we have examined agarose solutions in pure water or in the presence of 25 mM NaCl that were quenched to various temperatures in the range $20-43\,^{\circ}\mathrm{C}$.

Results reported here provide a detailed description of the competition between solution demixing and molecular cross-linking in the gelation process, as tuned by varying the quenching temperature at a fixed agarose concentration. The overall behavior is in good agreement with that observed at higher agarose concentration [15]. In that study, however, no spatial ordering signal was visible at the lowest temperature studied ($31.5\,^{\circ}\mathrm{C}$), indicating that at that higher agarose concentration, molecular cross-linking prevails over spinodal demixing. Here, at a low agarose concentration, the chosen range of quenching temperatures has made it possible to follow the gelation process under both regimes and clearly sort out the transition temperature between them.

Static light scattering results were fit to a newly developed model based on fractal aggregates surrounded by a polymer depleted region. The model was able to fit all our data over a wide range of q values using a consistent set of four parameters that could be followed over time as well. We found that there are two distinct regimes of aggregation depending on the depth of the temperature quench. Below about $30\,^{\circ}\mathrm{C}$, aggregates with characteristic sizes of about 0.5 μm and fractal dimensions of 3.0 rapidly form (within about 10 min) and appear to be frozen in time, with no further growth or intensity increase. Above this temperature, aggregates form more slowly in time, still have fractal dimensions above 2.6, but have characteristic sizes that increase with temperature up to about 5 μm or ten times larger than at lower temperature quenches. Surrounding the aggregates is a region roughly four times larger that is depleted of agarose polymer due to absorption within the aggregate over time. While the intensity amplitudes at the higher temperature quenches do not reach plateau values over the 15 h of our experiment, from Fig. 10 the final values appear to be independent of the quench temperature. A good point can be made of whether we are misrepresenting the correlation between different clusters with the depletion term in Eq. (5). As said above simple interaction terms (hard spheres) did not give satisfying fits. Neither was it sufficient to follow the approach of Giglio and co-workers [36], who represent the depletion term as a negative Fisher-Burford term. We therefore think that, while our model is consistent with all our data and the results are physically meaningful, we cannot exclude the possibility that our model is partially taking into account the correlation remnants left by the initial phase separation, frozen in by the competing cross-linking process.

The following working hypothesis emerges from our results for 0.5% agarose samples. When quenched below the spinodal curve (below $49.8\,^{\circ}\mathrm{C}$ at this concentration [20]), agarose rapidly demixes into domains of higher and lower agarose concentrations. Within the higher concentration domains fractal aggregates form, more rapidly at lower quench temperatures and also more rapidly in the presence of 25 mM NaCl, which apparently shields small residual charges on the agarose monomers.

When quenched below about $30\,^{\circ}\mathrm{C}$ in water, these aggregates form more rapidly, are more numerous, and have smaller characteristic dimensions and larger depletion regions than aggregates formed at higher quench temperatures. Once formed they appear to be frozen in position and in mass so that they scatter significantly less than those formed at higher quench temperatures eventually do. Once formed, these aggregates do not accrue further agarose polymer. Furthermore, under these conditions the even more rapid aggregate formation in the presence of salt produces faster initial intensity growth allowing an intensity plateau that is much higher, about a factor of 5, than in the absence of salt, to be reached before the aggregates are frozen. Below $30\,^{\circ}\mathrm{C}$ the cross-linking process dominates after an initial demixing to freeze the aggregates and prevent further demixing.

At higher quench temperatures, aggregates initially form more slowly, in smaller numbers and/or with lower densities, and with characteristic dimensions that are larger, but decrease slowly over the duration of the experiments. These samples are not frozen in time, but produce a logarithmically increasing scattered intensity due to the formation of more and/or denser aggregates. Scattered intensities at our highest quench temperatures are two orders of magnitude greater than at quench temperatures of $30\,^{\circ}\mathrm{C}$ or below. We interpret these results as indicating that above $30\,^{\circ}\mathrm{C}$ there is a steady absorption within the aggregates of neighboring polymer chains. The aggregates, in fact, very slowly decrease in characteristic dimension while absorbing more polymer, steadily increasing in density, resulting in a higher contrast and increasing scattered intensity. The region surrounding the aggregates becomes depleted of polymer, the aggregates expelling solvent to maintain their size as polymer chains are absorbed. This process may, in fact, be the initial stages of syneresis, in which solvent is expelled from a gel causing it to shrink. Normally syneresis leads to the macroscopic shrinking of a gel and the expulsion of solvent, while here this process is occurring locally within condensed aggregates and has no obvious macroscopic signature. The rate of absorption decreases inversely with time as polymer chains are depleted from the region surrounding the aggregates, leading to the logarithmic increase in scattered intensity. This implies that transport phenomena are still active at later time, an assumption that appears to be at odds with the progressive slowing down of diffusion. Actually, what is required is some degree of motion in the depletion region, where, due to low polymer concentration, cross-linking should be less relevant.

Because of the dynamic nature of the network at these higher quench temperatures, any initial differences due to the presence of salt are erased over time and the scattered intensity asymptotes in Fig. 10 are all close to the same value. Thus, in the absence of a mechanism for ''freezing in'' the

gel structure, the long-time M values from 0.5% agarose solutions appear to be essentially independent of quench temperature. Only at lower temperatures, where the aggregation is most rapid and frozen in, is the plateau scattered intensity below this common asymptotic value seen in Fig. 10.

On the macroscopic scale, elastic constants measured at low strains for 0.5% agarose samples quenched to the lower temperatures are significantly higher (over 200 times) than for those quenched to higher temperatures. Gels formed in the presence of salt have even slightly higher elastic constants. However these gels appear weaker in that when a strain scan is done about 3 h after quenching they require less strain (by a factor of 3–4) to be disrupted. Gels formed at higher temperatures are seen to be more resistant to breakage as the strain is increased. Lower temperature quenches lead to locally denser and smaller regions, with smaller depletion zones around these regions, and the number of interconnections between these regions can increase. This validates the higher G' values obtained at decreasing quench temperatures. At very low strain (4×10^{-3}), these samples exhibit much higher elastic moduli, but at strains roughly 50 times greater they macroscopically rupture. The increased rigidity of the system at the lower quench temperatures makes these gels more susceptible to rupture by applied strain. Samples quenched at higher temperatures are much less elastic at low strains, but somewhat more easily accommodate higher strains before being disrupted.

ACKNOWLEDGMENTS

We thank Dr. M. Manno for discussions and a critical reading of the manuscript. Technical support from F. Giambertone, G. La Gattuta, M. Lapis, and R. Megna is also acknowledged. One of us (J.N.) also acknowledges Union College for support.

[1] W. Burchard and S. B. Ross-Murphy, *Physical Networks* (Elsevier, London, 1988).
[2] A. H. Clark, in *Biopolymeric Mixtures*, edited by S. E. Harding, S. Hills, and J. R. Mitchell (Nottingham University Press, Nottingham, 1996).
[3] P. G. de Gennes, *Scaling Concepts in Polymer Physics* (Cornell University Press, Ithaca, 1979).
[4] C. J. Brinker and G. W. Scherer, *Sol-Gel Science* (Academic Press, San Diego, 1990).
[5] H. B. Boidar and S. Maity, Eur. Polym. J. **34**, 1361 (1998).
[6] J. Prost and F. Rondelez, Nature (London) **350**, 11 (1991).
[7] M. R. Mangione, D. Giacomazza, D. Bulone, V. Martorana, and P. L. San Biagio, Biophys. Chem. **104**, 95 (2003).
[8] P. L. San Biagio, D. Bulone, A. Emanuele, M. B. Palma-Vittorelli, and M. U. Palma, Food Hydrocolloids **10**, 91 (1996).
[9] M. Doi, *Introduction to Polymer Physics* (Clarendon Press, Oxford, 1996).
[10] *Reversible Polymeric Gels and Related Systems*, edited by P. S. Russo, ACS Symposium Series (ACS, Washington D.C., 1987), Vol. 350.
[11] P. L. San Biagio and M. U. Palma, Biophys. J. **60**, 508 (1991).
[12] P. L. San Biagio, D. Bulone, A. Emanuele, and M. U. Palma, Biophys. J. **70**, 494 (1996).
[13] M. Manno, A. Emanuele, V. Martorana, P. L. San Biagio, D. Bulone, M. B. Palma-Vittorelli, D. T. McPherson, J. Xu, T. M. Parker, and D. W. Urry, Biopolymers **59**, 51 (2001).
[14] M. Manno, C. Xiao, D. Bulone, V. Martorana, and P. L. San Biagio, Phys. Rev. E **68**, 011904 (2003).
[15] M. Manno, A. Emanuele, V. Martorana, D. Bulone, P. L. San Biagio, M. B. Palma-Vittorelli, and M. U. Palma, Phys. Rev. E **59**, 2222 (1999).
[16] R. Bansil, J. Lal, and B. L. Carvalho, Polymer **33**, 2961 (1992).
[17] S. C. Glotzer, M. F. Gyure, F. Sciortino, A. Coniglio, and H. E. Stanley, Phys. Rev. E **49**, 247 (1994).
[18] S. D. Hayward, D. V. Heermann, and K. Binder, J. Stat. Phys. **49**, 1053 (1987).
[19] Y. Liu and R. B. Pandey, J. Chem. Phys. **105**, 825 (1996).
[20] P. L. San Biagio, F. Madonia, J. Newman, and M. U. Palma, Biopolymers **25**, 2255 (1986).
[21] C. Araki and K. Arai, Bull. Chem. Soc. Jpn. **40**, 1452 (1967).
[22] P. L. San Biagio, J. Newman, F. Madonia, and M. U. Palma, in *Proceedings of Biomolecular Stereodynamics*, edited by R. H. Sarma and M. H. Sarma (Adenine Press, Albany, NY, 1986).
[23] A. Emanuele, L. Di Stefano, D. Giacomazza, M. Trapanese, M. B. Palma-Vittorelli, and M. U. Palma, Biopolymers **31**, 859 (1991).
[24] D. Bulone and P. L. San Biagio, Chem. Phys. Lett. **179**, 339 (1991).
[25] D. Bulone and P. L. San Biagio, Biophys. J. **68**, 1569 (1995).
[26] D. Bulone, J. Newman, and P. L. San Biagio, Biophys. J. **72**, 388 (1997).
[27] M. Leone, F. Sciortino, M. Migliore, S. L. Fornili, and M. B. Palma-Vittorelli, Biopolymers **26**, 743 (1987).
[28] P. N. Pusey and W. Van Megen, Physica A **157**, 705 (1989).
[29] F. Ferri, Rev. Sci. Instrum. **68**, 2265 (1997).
[30] D. Bulone, A. Emanuele, and P. L. San Biagio, Biophys. Chem. **77**, 1 (1999).
[31] P. L. San Biagio, D. Bulone, A. Emanuele, F. Madonna, L. Di Stefano, D. Giacomazza, M. Trapanese, M. B. Palma-Vittorelli, and M. U. Palma, Makromol. Chem., Macromol. Symp. **40**, 33 (1990).
[32] K. Binder and D. Stauffer, Phys. Rev. Lett. **33**, 1006 (1974).
[33] K. Kawasaki and T. Ohta, Prog. Theor. Phys. **67**, 147 (1982).
[34] T. Nicolai and W. Brown, in *Light Scattering: Principles and Developments* (Clarendon Press, Oxford, 1996).
[35] H. Furukawa, Adv. Phys. **34**, 703 (1985).
[36] M. Carpineti, M. Giglio, and V. Degiorgio, Phys. Rev. E **51**, 590 (1995).
[37] B. Chu, *Laser Light Scattering: Basic Principles and Practice* (Academic Press, New York, 1974).
[38] A. Emanuele and M. B. Palma-Vittorelli, Phys. Rev. Lett. **69**, 81 (1992).